

Gas/Solid Reactions with Nitrogen Dioxide[†]

Gerd Kaupp* and Jens Schmeyers

University of Oldenburg, FB 9-Organic Chemistry I, P.O. Box 2503, D-26111 Oldenburg, Germany

Received January 3, 1995[®]

Numerous gas/solid reactions of nitrogen dioxide with organic substrates are investigated preparatively and mechanistically. Gaseous NO₂ reacts with crystalline stable free radicals (nitroxyls **1**, verdazyl **6**) by electron transfer. The nitrite ions formed are irreversibly oxidized by NO₂ via oxygen atom transfer. Solid cation nitrates are formed quantitatively. Thione bonds of thiohydantoin **8** are transformed to carbonyl bonds with formation of sulfur and NO presumably via nitrites as intermediates. Hydantoin **13** oxygenates at its free 5-methylene group via C–H abstraction and nitrite or it undergoes N-1 nitration via N–H abstraction depending on the conditions. Both reactions proceed quantitatively. 1,3-Oxazolidin-2-one (**15**) gives N-nitration and N-nitrosation with the NO produced. Nonenolized crystalline barbituric acids **17** are quantitatively nitrated (C–N bond formation with radicals) at their methylene groups. 4-Hydroxybenzaldehyde (**19**) and vanilline (**22**) give quantitative aromatic nitration (C–N bond formation with arenes) without melting. All possible regioisomers are formed. Solid 9-methylanthracene (**26**) gives a quantitative yield of its 10-nitro derivative **27**. Crystalline anthracene (**28**) and gaseous NO₂ yield 3 primary products **29** (*cis*; *trans*) and the new dimeric product **30** as well as the stable secondary products **31** and **32**. The gas/solid tetranitration of tetraphenylethylene (**33**) is severely hindered by the water of reaction. However, a 95% yield of pure tetrakis(*p*-nitrophenyl)ethylene is obtained if the drying agent MgSO₄·2H₂O is admixed and the product **34** extracted. The gas/solid procedures avoid solvents and fuming nitric acid. They give pure products without necessity for recrystallization in most cases and they avoid wastes. Atomic force microscopy (AFM) measurements on prominent faces of single crystals of **1a**, **11a**, **28**, and **33** reveal phase rebuildings with well-directed long-range molecular transports. Nanoliquids were only present on (110) of **28**. The characteristic AFM features are correlated with known X-ray crystal structure data and compared with previous results. The shape of the features depends on the molecular packing in the crystal bulk and on the molecular shapes. Molecular interpretations of the AFM features are given.

Introduction

It is well recognized that NO₂ is a very reactive ubiquitous radical which takes part in atmospheric chemistry. Even atmospheric reactions of polycyclic aromatic hydrocarbons giving facile formation of mutagenic nitro derivatives have been analytically investigated.¹ Generally, exhaust gases from automotive or air traffic, power plants, and fires contain nitroarenes.² Even carbon black toners for photocopiers may contain hazardous nitro compounds.³ The formation of nitroarenes was modeled by using nitric acid or nitrogen dioxide. Such nitrations may proceed in the gas phase, in liquid aerosols, on particle surfaces, or in organic solution. While the particle reactions in the atmosphere are ill defined in terms of composition and physical state, we were interested in studying the interaction of nitrogen dioxide with pure crystalline materials on a preparative scale under strict exclusion of solvents or liquids. Such gas/solid reactions are highly useful in waste-free quantitative syntheses.⁴ Basic knowledge on the mechanisms of gas/solid conversions has recently been extracted from atomic force microscopy (AFM) investigations which shed new light on the importance of molecular packings for

the success of this unusual type of reaction. Thus, the availability of phase rebuilding mechanisms is an essential condition. Long-range transports give rise to now eight basic types of surface features which build up in a face selective manner and which have been classified according to their shapes.⁵

We report now on preparatively useful gas/solid reactions of NO₂ giving electron transfer, oxygen atom transfer, oxygenations, and N- and C-nitrations. Again, AFM and the use of X-ray crystallographic data provide valuable mechanistic information for the unusual reaction technique. Gas/solid runs are superior to solution runs with the same starting materials. Solvents are avoided, waste is avoided, quantitative reactions are obtained, and purification procedures are dispensable because in most cases only one product is formed.

Results and Discussion

Electron Transfer and Oxygen Atom Transfer of Nitrogen Dioxide. It appears that stable radicals exchange electrons with NO₂ to form nitrite salts (like

[†] Dedicated to Professor Glen A. Russell on the occasion of his 70th birthday.

[®] Abstract published in *Advance ACS Abstracts*, July 1, 1995.

(1) Pitts, J. N.; Van Cauwenberghe, K. A.; Grosjean, D.; Schmid, J. P.; Fritz, D. R.; Belser, W. L.; Knudson, G. B.; Hynds, P. M. *Science* **1978**, *202*, 515. See also ref 21.

(2) See: Nielsen, T. *Environ. Sci. Technol.* **1984**, *18*, 157.

(3) Rosenkranz, H. S.; McCoy, E. C.; Sanders, D. R.; Butler, M.; Kiriazides, D. K.; Mermelstein, R. *Science* **1980**, *209*, 1039.

(4) Kaupp, G.; Pogodda, U.; Schmeyers, J. *Chem. Ber.* **1994**, *127*, 2249 and earlier work cited therein. The question of long-term stability of host/guest inclusion systems for detoxification of air from organic solvent vapors under the influence of ubiquitous NO₂ has been investigated: Kaupp, G.; Pogodda, U.; Bartsch, K.; Schmeyers, J.; Ulrich, A.; Reents, E.; Juniel, M. *Minderung Organischer Luftschadstoffemissionen mittels Gas/Festkoerper-Reaktionen*, Bericht des Bundesministers fuer Forschung und Technologie, No. 01VQ9027, March 3, 1993; available from Technische Informationsbibliothek D-30167 Hannover, Welfengarten 1B, Germany.

(5) Kaupp, G.; Schmeyers, J. *Angew. Chem., Int. Ed. Engl.* **1993**, *32*, 1587. Kaupp, G. *Mol. Cryst. Liq. Cryst.* **1992**, *211*, 1.

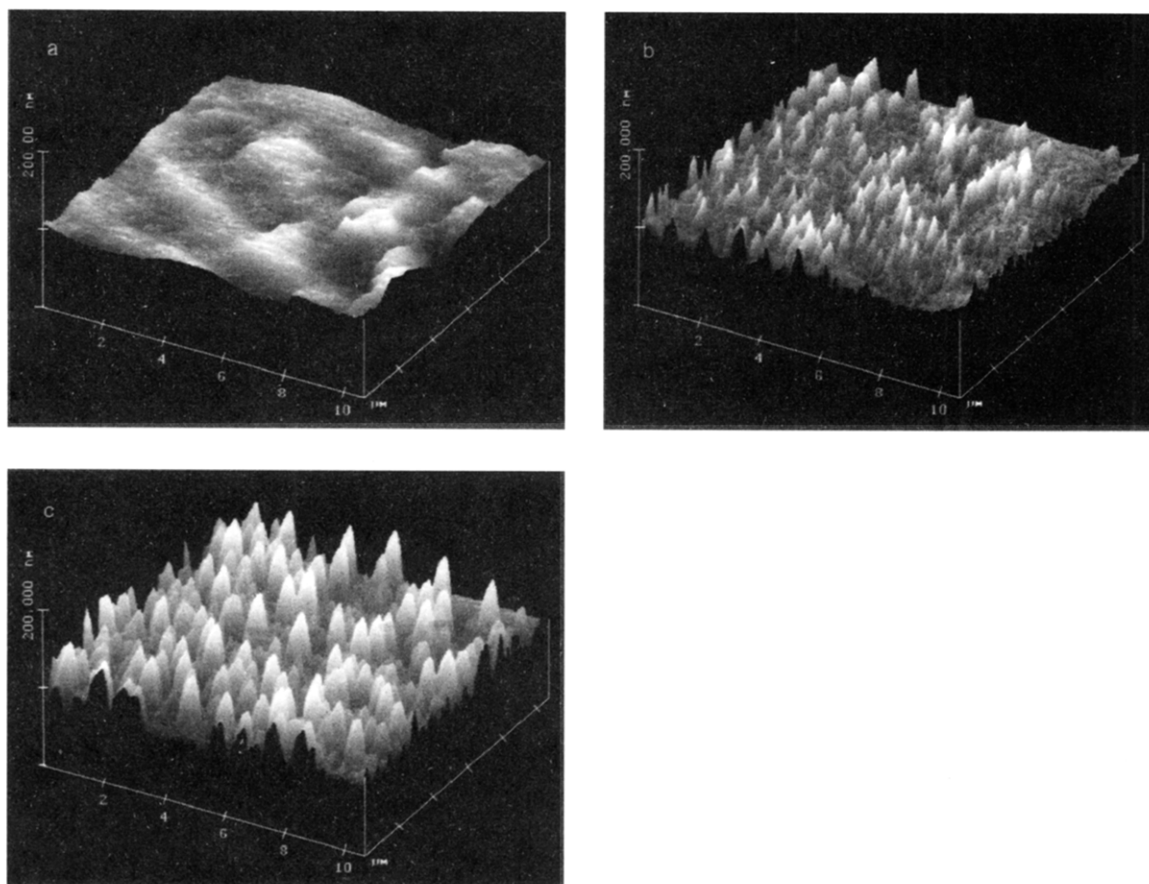
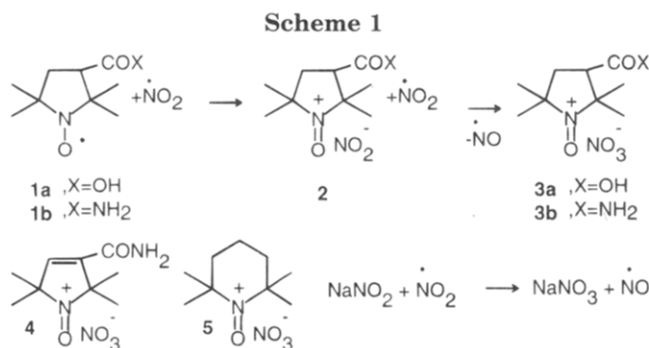


Figure 1. AFM surface of **1a** on (001): (a) natural face prior to reaction; (b) reaction features after one application of NO_2 ; (c) reaction features after two applications of NO_2 .



2). Such exchange may be reversible, however, as the nitrite anion is oxidized further by NO_2 via transfer of an oxygen atom to give the nonreducing nitrate anion; stable, even strongly oxidizing salts (like **3**) can be prepared. Thus, the reaction of NO_2 gas with the crystalline nitroxyl radical **1** leads quantitatively to NO and the nitronium nitrate **3** in analytically pure form in an hour or so. Similarly, **4** (from dehydro **1b**) and **5** (from tetramethylpiperidine-*N*-oxyl, TEMPO) can be obtained quantitatively by oxidation of the corresponding solid nitroxyls with NO_2 .

The oxoammonium nitrates **3** and **4** were previously obtained from dichloromethane solutions of the nitroxyls which were passed by 1% NO_2 in N_2 , filtered, and dried.⁶ However, the yields reached only 63 to 88%. The spectral data are identical with the solid state products. The

characteristic nitrate vibration bands are found at $1383\text{--}1384\text{ cm}^{-1}$, and the nitronium bands between 1600 and 1658 cm^{-1} in **3–5**. The ease of oxidation of nitrite to nitrate has also been shown with the gas/solid reaction of sodium nitrite with NO_2 , giving sodium nitrate and NO .

The conversion of **1a** on its natural (001) surface to give **3a** has been followed by AFM. Figure 1 shows that, starting from a weakly corrugated surface after application of gaseous NO_2 , volcano-type features are growing at random with heights approaching 100 nm. The edges on the features are obvious signs of crystallinity.

The reasons for this type of mechanism can be extracted from experimental facts. The mass increases by a factor of 1.25 when **1a** reacts to give **3a**. This increase cannot be accommodated by the initial crystal lattice. Clearly, a single crystal to single crystal conversion is impossible. Rather, a volume increase ensues and the crystal disintegrates on longer reaction. Furthermore, the crystal lattice does not impose steric hindrance to the reaction on (001). The molecular packing of racemic **1a** on (001), which is of the solid solution type ($Pnma$) in the enantiomer lattice ($P2_12_12_1$),⁷ is shown in Figure 2. It is easily seen that half of the molecules **1a** present their nitroxyl groups freely accessible on the surface. After electron transfer to the approaching NO_2 and after oxidation of the nitrite thus formed, the overall volume of the nitrate **3a** increases. The volume increase enforces molecular transports; the dense packing tells that these are only possible toward and above the (001) face. The

(6) Ma, Z.; Huang, Q.; Bobbitt, J. M. *J. Org. Chem.* **1993**, *58*, 4837. **4** from cyclohexane solution: Chov, S.; Nelson, J. A.; Spencer, T. A. *Ibid.* **1974**, *39*, 2356.

(7) Chion, B.; Lajzerowicz, J.; Bordeaux, D.; Collet, A.; Jacques, J. *J. Phys. Chem.* **1978**, *82*, 2682.

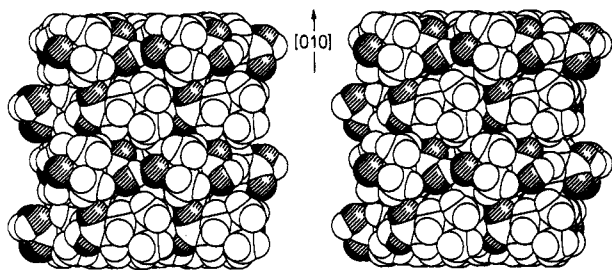
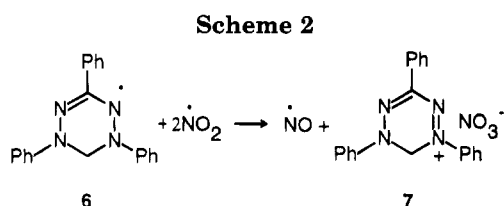


Figure 2. Stereoscopic space-filling model of the molecular packing of **1a** ($P2_12_12_1$) on (001), showing the accessibility of the nitroxyl-O for electron transfer to NO_2 when approaching the surface for half of the molecules: O, circles; N, hardly seen.

Table 1. Analytical Data of **3**, **4**, **5**, and **7** Generated by Gas/Solid Oxidation with NO_2

compd	dec ^a [°C]	mp [°C]	$\nu_{\text{R}_2\text{N}=\text{O}}$ [cm ⁻¹]	$\nu_{\text{NO}_3^-}$ [cm ⁻¹]	MS (CI) <i>m/e</i> (M ⁺)
3a	113	111–112 ^b	1658	1383	186
3b	118	138–140 ^b	1640	1384	186
4	<i>b</i>	128–130 ^b	1639	1383	184
5	117	110–120 ^c	1600	1384	
7	<i>b</i>	>85 ^c		1385	313

^a TGA inflection point. ^b Unsharp decomposition. ^c Slow decomposition with partial melting.



reaction can start everywhere at random; the generation of volcano-like hills is comprehensible. The second half of the molecules has to turn around prior to electron transfer, a process that is only possible because of the long-range transports that can be directly seen in Figure 1.

Nitrosonium salts like **3–5** are strongly oxidizing agents.⁸ Unlike the various salts that have been prepared by oxidations in solutions, our now quantitatively accessible nitrates are nonhygroscopic, stable at room temperature, and not shock sensitive. Their thermal decompositions are easily detected using TGA techniques. Thus, **3a** does not gain weight when left in moist air for 8 h. When heated, it decomposes sharply at 113 °C with 60% weight loss.

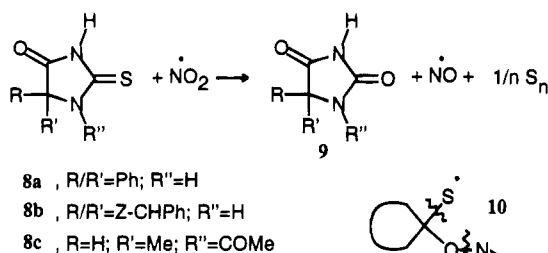
Clearly, the gas/solid technique for generating nitrosonium nitrates (oxoammonium nitrates) adds favorably to the versatility of these powerful oxidants.⁸ For oxidations which proceed at room temperature, their decomposition reactions at higher temperatures (see Experimental Section and Table 1) are not limiting.

Use of the electron-abstracting power of NO_2 followed by irreversible oxygen transfer to nitrite giving nitrate is obvious for the oxidation of further stable radicals. Thus, triphenylverdazyl (**6**)⁹ (Scheme 2) forms the stable violet salt **7** when gaseous NO_2 interacts. Again a stable

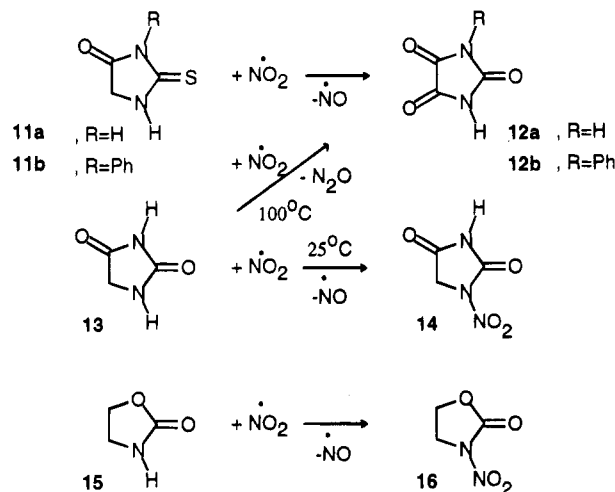
(8) Bobbitt, J. M.; Flores, M. C. L. *Heterocycles* **1988**, *27*, 509. Bobbitt, J. M.; Flores Guttermuth, M. C.; Ma, Z.; Tang, H. *Ibid.* **1990**, *30*, 1131. Ma, Z.; Bobbitt, J. M. *J. Org. Chem.* **1991**, *56*, 6110. Golubev, V. A.; Voronina, G. N.; Rozantseo, E. G. *Bull. Acad. Sci. U.S.S.R. Chem. Ser.* **1970**, *19*, 2449.

(9) Kuhn, R.; Trischmann, H. *Monatsh. Chem.* **1964**, *95*, 457. Williams, D. E. *Acta Crystallogr.* **1973**, *B29*, 96.

Scheme 3



Scheme 4



non hygroscopic nitrate is obtained in a quantitative gas/solid process. Hitherto, **7** has been studied in dilute solutions after oxidation of **6** with various agents.¹⁰ Its easy preparative access puts it now on the list of promising oxidation agents.

Gas/Solid Oxygenations with Nitrogen Dioxide.

While accepting an electron is the simplest reaction of NO_2 , this powerful radical reagent may also add to thione bonds with one of its oxygen atoms, leaving carbonyl groups after proper cleavage reactions. It can be shown that solid thiones are converted to solid carbonyl compounds under the action of gaseous NO_2 . Such transformations have been performed previously with nitric acid.¹¹ Again the gas/solid technique has important advantages. The yields are quantitative (Scheme 3). The solid sulfur can be easily sublimed off. No waste is formed. The product NO may be recycled by reoxidation to NO_2 with oxygen. The mechanism is traced in formula **10**. The wealth of oxygenations of easily accessible thiohydantoin **8** stems from the fact that the product hydantoin are not easily obtained by other techniques. No nitration at the N-3 of **8** is observed.

If the 5-position in thiohydantoin is unsubstituted as in **11**, both the methylene and the thione groups are oxygenated by NO_2 . Thus, solid **11a** and **11b** provide oxygenation in both the 2- and 5-positions, giving the parabanic acids **12** (Scheme 4). Clearly, the radicals formed by methylene hydrogen abstraction to NO_2 are stabilized by the thione group. Subsequent addition of NO_2 to form a labile 5-nitrite as an intermediate is an

(10) Lazar, M.; Rychly, J.; Klimo, V.; Pelikan, P.; Valko, L. *Free Radicals in Chemistry and Biology*; CRC Press: Boca Raton, FL, 1989; p 98.

(11) Biltz, H. *Chem. Ber.* **1909**, *42*, 1792. Shirai, H.; Yashiro-Nagoya, T. *Shiritsu Daigaku Yakugakubu Kiyo* **1959**, *7*, 42; *Chem. Abstr.* **1960**, *54*, 3388h.

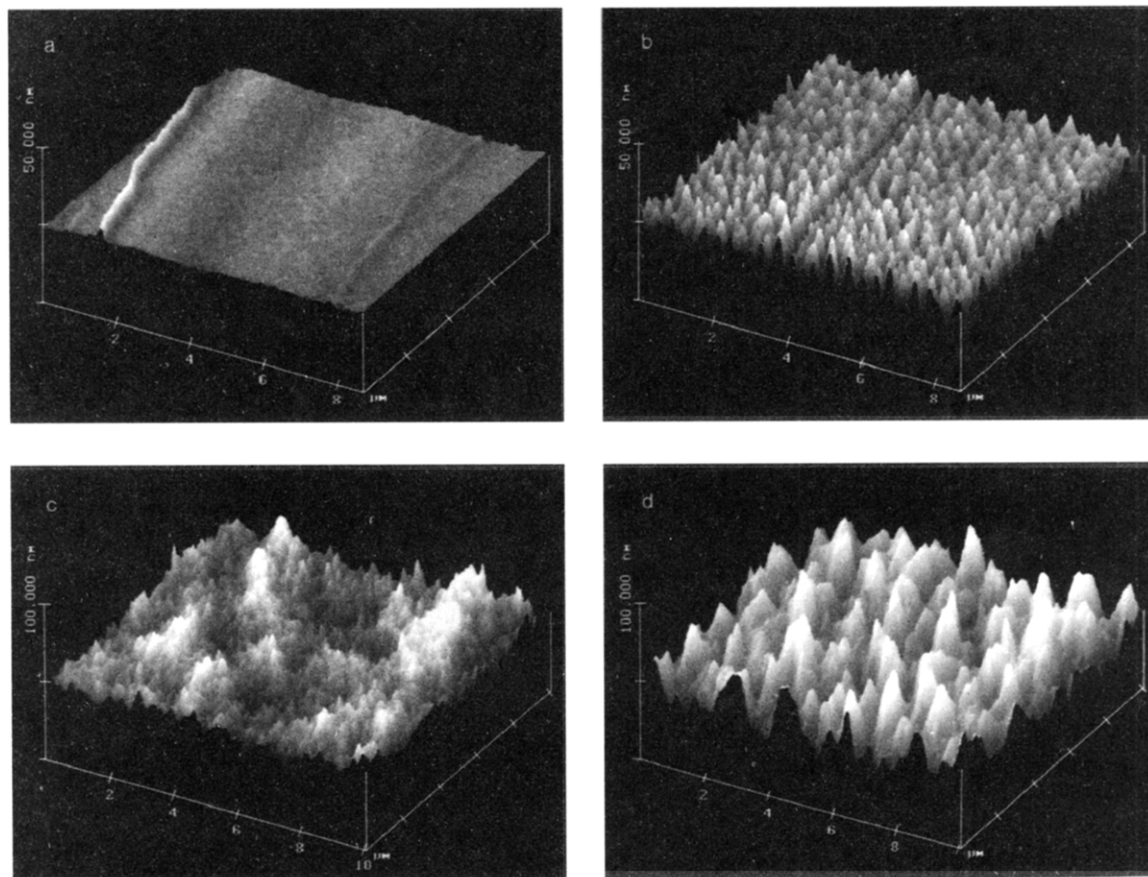


Figure 3. AFM surfaces of **11a** ($P2_1/c$); (a) $(10\bar{2})$ fresh; (b) $(10\bar{2})$ after a second treatment with gaseous NO_2 ; (c) (110) after one treatment with NO_2 ; (d) (110) after a second treatment with NO_2 .

obvious way to the 5-carbonyl group in **12** (leaving behind N_2O and H_2O as stoichiometric products). In an apparently slower reaction, the thione group of **11** is oxygenated via an intermediate of type **10**. Evidence for that sequence of events is provided by the reaction of hydantoin **13** with NO_2 . Compound **13** is no intermediate in the oxygenation of **11a** (both **11a**¹² and **13**¹³ are *not enolized* in the crystalline state). Heating to 100°C is required for the reaction of NO_2 with crystalline **13** to give the product **12a**. If, however, crystalline **13** is reacted with NO_2 at room temperature, a quantitative yield of the *N*-nitro compound **14** is obtained (in addition to H_2O and NO), which decomposes on heating but does not form significant quantities of **12a**. Well-balanced energetic differences and product stabilities determine the outcome of the quantitative reactions. The generality of the new technique for the synthesis of *N*-nitro amides was tested with solid oxazolidin-2-one (**15**) which gives an 80% yield of **16** simply by reaction with gaseous NO_2 . However, unlike **13**, solid **15** reacts with the stoichiometrically generated NO , yielding 20% of the byproduct *N*-nitrosooxazolidin-2-one. It should be pointed out that our new technique avoids the use of fuming nitric acid¹⁴ and that reduction of **14** yields 1-aminohydantoin which is an important intermediate in the preparation of several

hydantoin pharmaceuticals.¹⁵ Thus, our particularly clean gas/solid technique offers synthetic promise.

An AFM study of the multistep reaction of **11a** with NO_2 was undertaken to gain further insight into the reasons for its gas/solid reactivity. Both the natural (110) face and the $(10\bar{2})$ cleavage plane can be probed, and the molecular packing has been pictured stereoscopically.⁵ The phase rebuilding mechanism is different on the different faces, as can be seen by the unlike features in Figure 3. Even in this complicated multiple reaction the crystal bulk controls the distinct long-range molecular transports up to distances of more than 50 nm. The freshly cleaved $(10\bar{2})$ plane is very smooth. Upon an initial treatment with NO_2 , only small hills and depressions ($1.2/\mu\text{m}^2$, around 3 nm high, not shown) are formed. It is the second treatment with NO_2 that creates the very regular egg-box type features (both volcanos and craters) of Figure 3b ($6.0/\mu\text{m}^2$, typically 13 nm high).

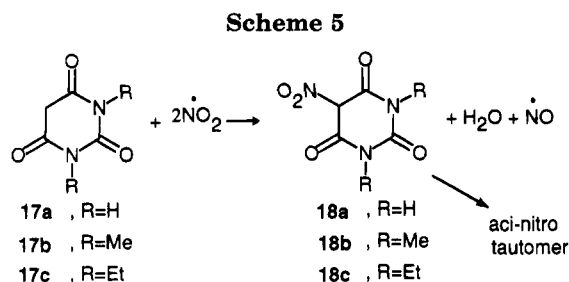
The features found are completely different on the rougher natural (110) face (initial surface not shown, cf. image in ref⁵). Highly structured wide hills have formed which on further reaction grow together to less structured and more uniform hills of considerable height (Figure 3c,d). Some preferred orientation is seen across the surface of Figure 3d. This orientation follows roughly

(12) Walker, L. A.; Folting, K.; Merritt, K. L. *Acta Crystallogr.* **1969**, B25, 88.

(13) Korshunov, A. V.; Volkov, V. E.; Lebedev, R. S.; Yukhimets, V. N. In Sechkarev, A. V., Kurshunov A. V., Eds.; *Vopr. Mol. Spectrosk.* **1974**, 308. Nauka, Sib. Otd., Novosibirsk, USSR; *Chem. Abstr.* **1975**, 82, 85967. Saito, Y.; Machida, K. *Bull. Chem. Soc. Jpn.* **1978**, 51, 108.

(14) Stuckey, R. E. *J. Chem. Soc.* **1947**, 331.

(15) Use for nitrofurantoin: Hayes, K. J. (Eaton Laboratories, Inc.), U.S. 2,610,181, 1952; *Chem. Abstr.* **1953**, 47, 6980i. Cadwallader, D. E.; Jun, H. W. *Anal. Profiles Drug Subst.* **1976**, 5, 345. Chamberlain, R. E. *J. Antimicrob. Chemother.* **1976**, 2, 325. Use for dantrolene: Norwich Pharmacal Co. NL 6612588, 1967; *Chem. Abstr.* **1967**, 67, 108657s. Oleinik, A. F.; Andreeva, N. I.; Syubaev, R. D.; Golovina, S. M.; Vozyakova, T. I. *Khim. Farm. Zh.* **1984**, 5, 561; *Pharm. Chem. J.* **1984**, 5, 310.

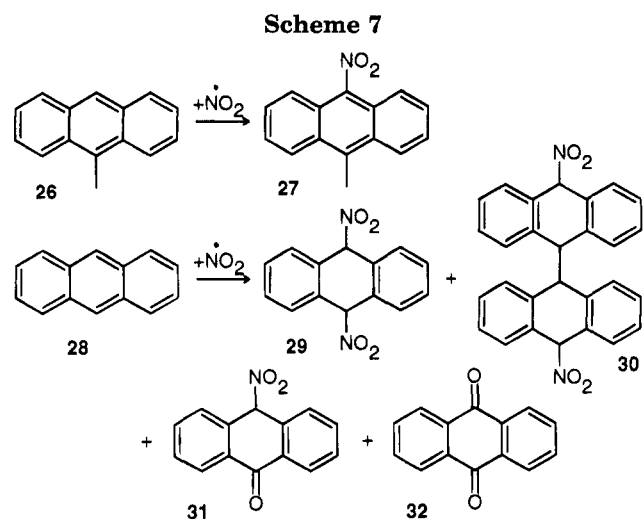
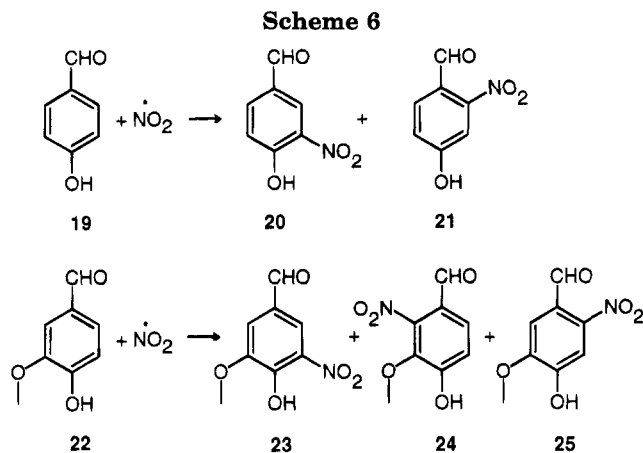


the direction of the (10 $\bar{2}$) cleavage plane, cutting (110) at an angle of 66°.⁵

The features of Figure 3 can be compared with those formed in the gas/solid aminolysis of **11a** with methylamine.⁵ Those are different from the present ones on (10 $\bar{2}$) (volcanos) and on (110) (heights and valleys, though in the same preferred orientation). Clearly, these observations show that the same crystal bulk of **11a** leads to different feature types while controlling the long-range molecular movements, if the chemistry is different. Thus, both the bulk structure and the form of the product molecules decide on the shape of the features. Obviously, some similarity of the features is preserved. It must be concluded that on volume increase due to chemical reaction the molecular transports follow similar rules as in ref⁵, the molecules being 66° steep under (110) in layers parallel to the (10 $\bar{2}$) cleavage plane. Importantly, the stability of the AFM surfaces during more than 10 scans shows that no organic nanoliquid is involved.¹⁶

Gas/Solid Nitrations with Nitrogen Dioxide. Nitro compounds ensue from reactions of NO₂, if it reacts at its nitrogen atom. Such radical nitrations of methylene groups are preceded by hydrogen atom abstraction, whereas double bonds may react by direct addition of NO₂. Thus, crystalline heterocyclic 1,3-dicarbonyl compounds and arenes are obvious starting materials for nitrations with gaseous NO₂. Competition of oxygenation is to be expected if the attack of NO₂ proceeds with its oxygen atoms (cf. the reactions of **11** and **13**) in the absence of nitrite to nitro rearrangement or by secondary reactions of intermediates.

The nitration of barbituric acids with fuming nitric acid¹⁷ can be improved with gas/solid techniques. From **17a** or disubstituted **17b,c** the 5-nitro compounds **18** (dilituric acids) are formed quantitatively (Scheme 5). **17a** is *not enolized* in the crystalline state.¹⁸ Therefore the 5-nitration of **17a** (and most likely also the nitrations of **17b,c**) must run via initial hydrogen atom abstraction by NO₂ to form a highly stabilized radical. Successful combination of this radical with NO₂ chooses binding to N but not to O, to give the 5-nitro compound **18a**. HNO₂ is formed in the primary step and decomposes to NO₂, NO, and H₂O. The water of reaction is partially retained in the solid products **18**, but it can be removed at 80 °C under vacuum. Product **18a** has been shown to exist as its *aci-nitro* tautomer in the crystalline state.¹⁸ While the yield in the solution nitration of **17a** with fuming nitric acid is described to be 85–90% (worse with **17b,c**),¹⁷ our yield is quantitative in all three cases. The



gas/solid processes are easily handled and proceed without waste formation. The NO formed is simply oxidized with O₂ to give NO₂ for further use.

Solid phenols like 4-hydroxybenzaldehyde (**19**) or vanillin (**22**) react with gaseous NO₂; however, several substitution products occur in quantitative radical reactions without liquefaction. Clearly the selectivities are different from solution nitrations. However, chromatographic separations are necessary for product isolation. In liquid phase nitrations of **19**, only the 3-nitro product **20** was formed with 63%¹⁹ and 93%²⁰ yield. The isomer **21** had not previously been reported (Scheme 6).

Solid polycyclic arenes may also be nitrated with NO₂ without melting. Environmental studies^{1–3} had not specified the physical states but aimed to detect possible artifacts by ubiquitous NO₂.

It is possible to react arene crystals with NO₂ gas on a preparative scale. Thus, the 9% yield of solution state nitration²¹ of 9-methylanthracene (**26**) was raised to 100% simply by reaction of crystalline **26** with gaseous NO₂.

In the case of crystalline anthracene (**28**), several products (**29–32**, Scheme 7) form and this behavior warrants a look for the underlying reasons. Solution state nitrations of **28** with nitric acid or N₂O₄ provided

(16) Kaupp, G. *Mol. Cryst. Liq. Cryst.* **1994**, *242*, 153; *J. Vac. Sci. Technol.* **1994**, *B12*, 1952.

(17) Biltz, H.; Sedlatschek, K. *Chem. Ber.* **1924**, *57*, 342. Hartmann, W. W.; Sheppard, O. E. *Org. Synth.* **1932**, *12*, 58.

(18) **17a**: Bolton, W. *Acta Crystallogr.* **1963**, *16*, 166. **18a** anhydrous: Bolton, W. *Ibid.* **1963**, *16*, 950. **18a** trihydrate: Craven, B. M.; Martinez-Carrera, S.; Jeffrey, G. A. *Ibid.* **1964**, *17*, 891.

(19) Zikolova, S.; Sabeva, A.; Bashikarova, A.; Konstantinova, R.; Zhelyaskova, M. *Tr. Nauchnoizsled. Khim.-Farm. Inst.* **1984**, *14*, 13; *Chem. Abstr.* **1985**, *103*, 71016r.

(20) Cornelis, A.; Laszlo, P.; Pennetreau, P. *Bull. Soc. Chim. Belg.* **1984**, *93*, 961.

(21) Paputa-Peck, M. C.; Marano, R. S.; Schuetzle, D.; Riley, T. L.; Hampton, C. V.; Prater, T. J.; Skewes, L. M.; Jensen, T. E.; Ruehle, P. H.; Bosch, L. C.; Duncan, W. P. *Anal. Chem.* **1983**, *55*, 1946.

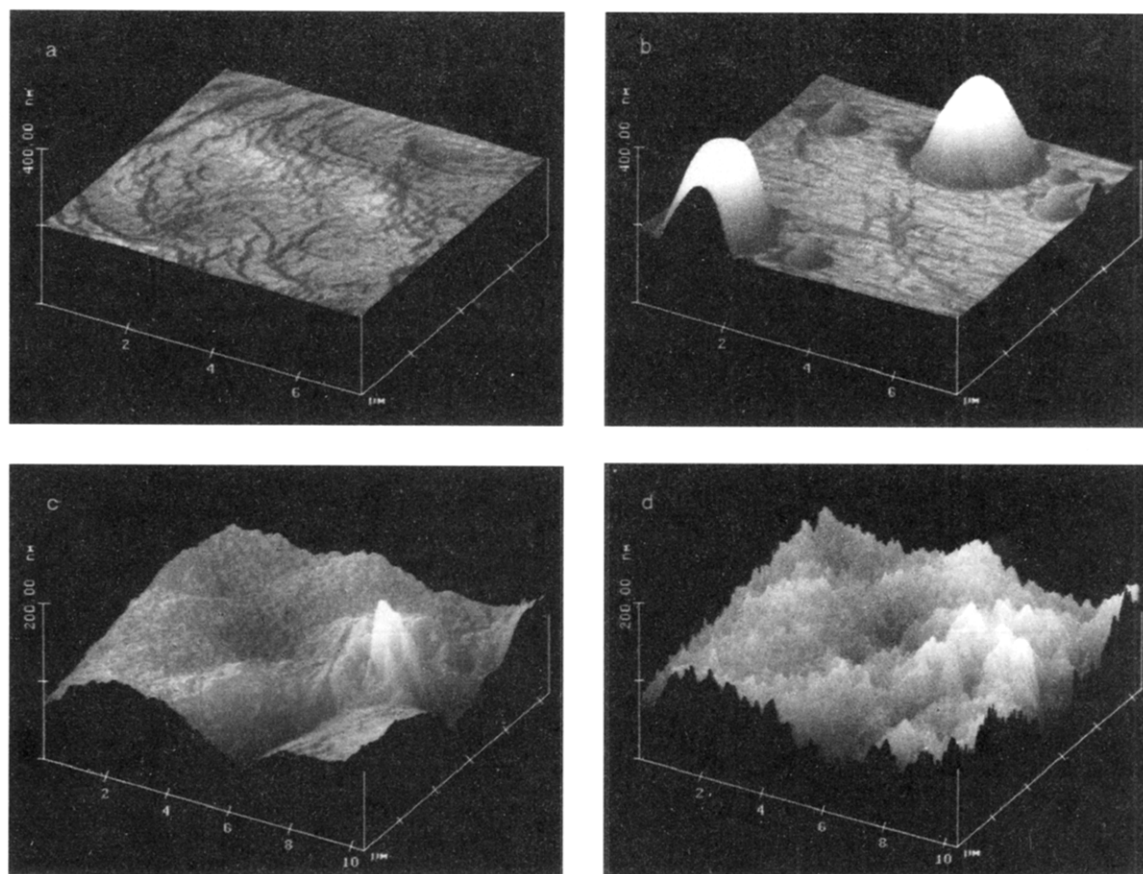


Figure 4. AFM surfaces of anthracene **28**: (a) (001) fresh; (b) (001) after two applications of NO₂; (c) (110), first scan after one NO₂ application; (d) change of the surface c after 10 AFM scans at 4.73 Hz scanning rate.

numerous products including **29**, **31**, and **32**,²² but not the dimeric product **30**. The variability must derive from both N and O attack of NO₂ to the 9/10 positions of **28** and from secondary reactions of the intermediates. Therefore, the advantage of orientation specificity found with **1**, **11**, **13**, **15**, **17**, and **26** (also reaction-type specificity with **19** and **22**) is lost with anthracene. While **29** (*cis* and *trans*) and **30** are primary products, **31** and **32** must be secondary ones whose proportions increase at the expense of the primary products at higher conversions. At 25 °C and 28% conversion, the proportion of *trans*-**29**/*cis*-**29**/**30**/**31**/**32** is 1/1.2/1.5/3.2/0.2. Decreasing the temperature to -10 °C disfavors **31** in a much slower overall reaction (1/1.1/1.6/1/0.9 ratio at 35% conversion). After complete conversion of **28** at room temperature, 75% **31**, 20% **32**, 4% *cis*-**29**, and almost no dimeric **30** are obtained. Thus, the course of reaction is different from all nitrations in solution. The dimeric product **30** is a consequence of the high concentration of **28** in the crystal which facilitates the trapping of the primary radical (after addition of NO₂ to **28**) by **28** in competition to NO₂. Several mechanisms for the formation of **31** and **32** may be devised (also those including nitrites); however, solvolysis conditions are required for the formation of anticipated 9-nitroanthracene and such conditions are not available in the solid state reaction.

The nonselective behavior of **28** is unusual for gas/solid reactions. Further information is gained from AFM investigations. They reveal that apparently different

reactions occur on different faces of crystalline **28**, which of course cannot be differentiated in preparative runs with multicrystalline materials. The molecular packing on two prominent faces of **28** has been stereoscopically depicted elsewhere.²³ Thus, on (001) the 9,10 positions of **28** are inaccessibly buried even in the upmost layer, whereas on (110) the 9 carbons of **28** are freely accessible. The phase rebuildings²³ in the AFM images of Figure 4 reflect the consequences of that difference. On very flat (001), the reaction is strongly hindered due to the molecular packing. Reaction starts only at isolated points where the gas may attack the crystal at some defect, and very large isolated volcano islands keep on growing concentrically while material moves out of the lattice above the top level of the (001) face. Even molecular terrace steps are retained between the islands (Figures 4a,b). Importantly, the surface is stable and shows no indication of a nanoliquid.¹⁶ This situation changes drastically if the more corrugated²³ (110) face (the unreacted surface had a landmark peak to the right; not shown) is probed. Now the reactions start so rapidly that only ill-defined surface changes occur and more importantly that a nanoliquid is formed by local melting point depression due to the numerous products formed. Organic nanoliquids can be readily detected by ordinary contact AFM.¹⁶ No NO₂ reagent was present in the time lag between the images of Figures 4c and 4d. The only distinctions were 10 continuous AFM scans with a nonscraping tip^{4,16,23} which transported moderately viscous liquid over the surface and apparently provoked a lot of

(22) Squadrito, G. L.; Fronczek, F. R.; Watkins, S. F.; Church, D. F.; Pryor, W. A. *J. Org. Chem.* **1990**, *55*, 4322 and references cited therein.

(23) Kaupp, G.; Plagmann, M. *J. Photochem. Photobiol. A: Chem.* **1994**, *80*, 399.

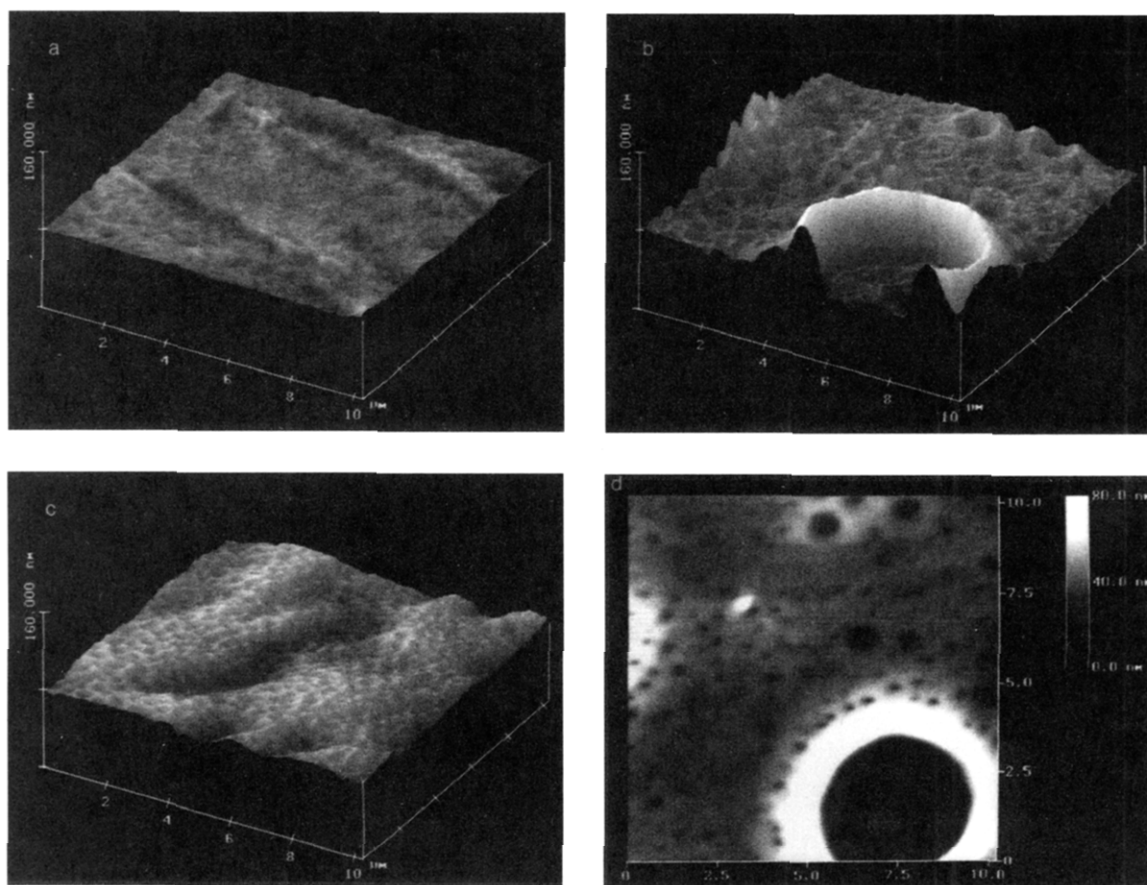
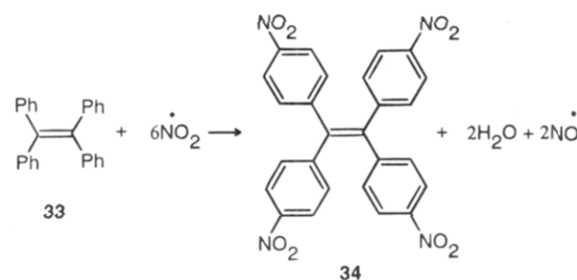


Figure 5. AFM surfaces of tetraphenylethylene (**33**): (a) fresh natural (10 $\bar{1}$) surface; (b) and (d) (10 $\bar{1}$) surface after 10 min treatment with 0.2 bar NO₂; (c) (10 $\bar{1}$) surface after 20 min treatment with 0.2 bar NO₂.

local recrystallizations on it and at the landmark.¹⁶ One has to conclude that initially the product composition on (110) is more complex than that on (001). The possibility of different reactions on different faces should be taken into account in all solid state reactions with more than one product, even if no submicroscopic nanoliquid occurs. Direct spectral evidence for such behavior is expected from scanning near-field optical microscopic (SNOM) studies.²⁴ For **28** and NO₂, one has to conclude that the gas/solid process soon resembles a liquid state reaction because of the nanoliquid formed.

An exciting possibility is the multiple nitration of tetraphenylethylene (**33**). Its double bond is of low reactivity, and various nitration techniques using nitric acid or dinitrogen tetroxide led to tetrakis(*p*-nitrophenyl)ethylene, the structure of which had been unambiguously proven in 1959.²⁵ The yields varied from 65 to 75% under optimized conditions. We were intrigued in trying 4-fold nitration under gas/solid conditions, a possibility that was facilitated by the long-range molecular movements. Thus, the phase rebuilding^{4,5,16,23} creates the possibility of reaching each *para* position in every molecule by gaseous NO₂, and a 95% yield of **34** is obtained after extraction, if the water of reaction is removed by the admixed drying agent MgSO₄·2H₂O (Scheme 8). In the absence of drying agent, the reaction is severely hindered by liquid water condensing on the crystals, and a mixture of mono-, tri-, and tetra-*p*-nitro products is obtained. Apparently, the approach of the gas is impeded by the wetting. Despite the technical requirement for re-

Scheme 8



moval of the water, the gas/solid technique for the preparation of **34** is by far superior to the liquid phase nitrations. This fact is evident if the properties of the wastes produced and the ease or cost of operation are compared. In the solid state nitration, the pure product is obtained at room temperature without the need for recrystallization.

It is of interest to know if the crystal structure of **33** still governs the feature-forming phase rebuilding in the 4-fold nitration. The water formed will rapidly evaporate from the surface of single crystals while probing it with the AFM. Anyhow, as it does not dissolve **33** and its nitration products, it will not deteriorate the AFM surface (as do organic liquids, see Figure 4) when some of it remains. The AFM measurements show a rather flat initial (10 $\bar{1}$) surface. After 10 min in an atmosphere of NO₂ at 0.2 bar and evaporation, regular craters with nicely developed rims of very different sizes are spread all over the surface. The large flat bottom crater of Figure 5b has a rim to rim diameter of 5 μ m, a height of 65 nm, and slope of 10°. At the left side of the image

(24) Kaupp, G. *Adv. Photochem.* **1995**, *19*, 119.

(25) Gorvin, J. H. *J. Chem. Soc.* **1959**, 678.

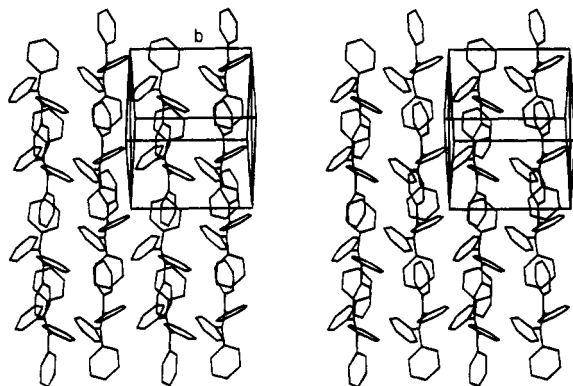


Figure 6. Stereoscopic wire model of the molecular packing of **33** ($P2_1$) on $(10\bar{1})$ showing molecular rows in three almost orthogonal directions; the hydrogens are omitted for clarity.

the spur of another big crater can be seen. The top view (Figure 5d) shows the different sizes of the craters even more clearly. The dark hole is 60 nm deep. Upon further reaction, the features flatten out (Figure 5c). Such behavior is an indication for completion of the reaction with phase transformation to give the product lattice.^{4,16,23} The crater formation requires concentric movements as the volume of the product molecules **34** increases. Such concentric behavior on $(10\bar{1})$ with upward transport above the initial face is comprehensible from the crystal structure²⁶ (Figure 6). The average molecular planes are normal to the face.

The molecules form interlocked rows in three almost orthogonal directions. The development of concentric lateral movements within the lattice of **33** may be traced as follows: The molecules have a limited possibility for partial turns within a layer around their axis perpendicular to the $(10\bar{1})$ face. They will make the turn if they become larger because of nitration. After a clockwise (cw) turn of a first molecule, its encounter with the neighbor molecule in the next row will force this second one to make a similar turn counterclockwise (ccw) and provoke the encountered third molecule in the third row to turn cw with encounter of a fourth molecule in the middle row to enforce a ccw turn also filling the gap opened by the first molecule. Thus, a cyclic array is formed which can serve as a center of preferred reaction at all four *para* positions of each molecule. From there molecules will move upward as increasing space requirement demands because the nitrated molecules are larger. Neighboring rows will participate from the beginning and thus increase the diameter of the crater and the height of its circular wall. While the conditions for the formation of the very large craters which are spread over the whole surface area at average distances of about 30 μm cannot be assessed, it should be noted that their sizes appear to depend on more subtle local reaction conditions. Thus, some crystals gave even larger craters whereas others stopped at around 1 or 2 μm diameters. Anyway, there can be no doubt that the bulk of the starting crystal determines the type of the phase rebuilding (crater features), exhibiting well-directed long-range molecular transports without liquefaction. At longer reaction periods when the proportion of **34** has increased, it is to be assumed that phase rebuilding switches over to phase transformation,^{4,16,23} forming the lattice of **34** with loss of the intermediate features. The stability of the AFM

surfaces in Figure 5 at multiple scans proves that no nanoliquid organic phase is present on the surface.

Conclusions

Virtually all primary reaction types of NO_2 with organic substrates (electron transfer, oxygen atom transfer, H-abstraction, and O/C- and N/C-bond formation) have been demonstrated for gas/solid reactions. In most cases, preparatively useful quantitative reactions were obtained in reasonable times without the need of grinding the starting crystals. The reactions are easily run. They avoid waste (only the undesirable N_2O liberation in the oxygenation reactions of **11** and **13** will ask for some technical expenditure) as well as costs and efforts of purification. Thus, gas/solid reactions of NO_2 recommend themselves for use in improved syntheses. As NO_2 reacts rapidly it can be envisioned that gas/solid reactions might be also of use for removing NO_x from (cold) stack or exhaust gases. While NO is readily oxidized by O_2 to give NO_2 , its gas/solid potential is more limited than that of NO_2 . The only successful gas/solid reaction of NO with the substrates of this work was the N-nitrosation of **15**. However, the crystals liquefied in the reaction with neat NO. The other substrates of this work did not change in an NO atmosphere. While solid secondary amines might be obvious candidates for gas/solid nitrosations with NO gas, the expected nitrosamines are known for their cancerogenic properties. Therefore, reactions of secondary amines with NO_2 have been postponed because a mixture of *N*-nitro and *N*-nitroso compounds is to be expected. The amide **15** behaved that way.

Gas/solid techniques are by far superior to solution reactions in all reported examples. No solvent is needed, waste is avoided or minimized, pure single products are formed quantitatively in most cases, and, if more than one product occurs, the workup is facilitated and less expensive than in corresponding solution reactions. Thus, there should be synthetic promise.

Experimental Section

All crystalline materials for the preparative runs were purchased from Aldrich and used without purification or grinding. Single crystals of the nitroxy **1a**, thiohydantoin (**11a**), anthracene (**28**), and tetraphenylethylene (**33**) were grown from saturated solutions in ethanol, acetone, ethanol (for (001); 1,2-dichloroethane for (110)), and acetonitrile, respectively. The AFM techniques and reliability tests of this method have been thoroughly described elsewhere.^{4,16,23} Only nonscrapping Si_3N_4 tips^{4,16,23} have been used. After scanning of a single crystal of **1a**, **11a**, and **28** on the proper face, the head was removed and 1 mL of 0.2 bar NO_2 in air was slowly (10–20 s) pushed out of a syringe with its needle end held at about 1 cm from the crystal surface. Excess NO_2 was blown away after 1 min with a stream of air, and after reinstallation of the AFM head, the scanning was taken up within 5 to 10 min at the previous site of the crystal. Crystals of **33** reacted more slowly. They were removed from the AFM stage together with their support, placed in a flask, evacuated, and treated with NO_2 gas at a pressure of 0.2 bar for 10 or 20 min. After evacuation, AFM measurement was done as closely as possible to the original site as judged with a telescope viewing the unchanged shape of the crystal. The crystal orientation had been reinstalled as previously marked on the stage. In all cases AFM measurements were extended to other sites of the same face to prove uniformity of the features. All AFM measurements were repeated at least twice with other crystal species of the same compound to secure the reproducibility of the features.

(26) Hoekstra, A.; Vos, A. *Acta Crystallogr.* **1975**, *B31*, 1716.

Preparation of the Oxoammonium Nitrates 3 and 4.

An evacuated 100 mL flask was filled with dinitrogen tetroxide (N_2O_4) from a lecture bottle to a pressure of 650 mbar (296 mg, 6.4 mmol NO_2 , mostly as its dimer N_2O_4). The sampling flask was connected to an evacuated 1 L flask; 500 mg (2.7 mmol) of **1a**, **1b**, or the dehydrated nitroxyl **1b'** (synthesis of **4**) was evacuated in a 10 mL flask, cooled to 5 °C (the synthesis of **3a** can be also performed at room temperature without melting and with equal success), and connected at a vacuum line to the flasks containing NO_2 . After 1 h, excess NO_2 and NO were condensed in a cold trap at 77 K, with removal of the cooling bath for 1 h to expel all NO_2 dissolved in the solid product; 665 mg (100%) of the product **3a**, **3b**, or **4** was obtained. The products are not hygroscopic and not shock sensitive when milligram quantities of them are hit with a hammer on an anvil.

The TGA of **3a** (10 K/min) shows a sharp decomposition with loss of 61% of the weight at 113 °C. At rt no weight increase was detectable within 8 h in moist air (at 70% relative humidity).

Preparation of the Oxoammonium Nitrate 5. The precursor TEMPO (tetramethylpiperidine-*N*-oxyl) was similarly reacted in 2 g quantities at -10 °C with NO_2 at an initial pressure of 0.03 bar and refill of the brown gas when consumed and evacuation until the theoretical weight increase was achieved (about 12 h).

Solid State Oxidation of Sodium Nitrite. Commercial NaNO_2 (200 mg, 2.9 mmol) was reacted in a vacuum system with 6.4 mmol of NO_2 at an initial pressure of 0.2 bar for 24 h at room temperature; 245 mg (100%) of NaNO_3 with its characteristic nitrate vibration band at 1384 cm^{-1} (KBr) was obtained.

Oxidation of Triphenylverdazyl (6) To Give the Nitrate 7. Similarly to the preparation of **3**, 200 mg (0.64 mmol) of solid triphenylverdazyl (**6**) was oxidized with gaseous NO_2 (3.2 mmol) at an initial pressure of 0.2 bar at 0 °C in quantitative yield. UV (acetonitrile): λ_{max} (log ϵ) 244 (4.05), 313 (4.14), 544 nm (3.88). Anal. Calcd for $\text{C}_{20}\text{H}_{17}\text{N}_5\text{O}_3$: C, 63.99; H, 4.56; N, 18.66. Found: C, 64.17; H, 4.78; N, 18.38.

Formation of Hydantoins 9. Compounds **8a-c** (500 mg, 1.87–2.45 mmol) were evacuated in a 100 mL flask and reacted with 6.4 mmol of NO_2 at an initial pressure of 0.2 bar for 6 h. The remaining NO_2/NO mixture was condensed in a cold trap at 77 K; the sulfur in the solid product was sublimed off at 100 °C and 5×10^{-4} Torr. The yields of spectroscopically (^1H and ^{13}C NMR) pure products **9** were quantitative.

9a: mp 295–297 °C, lit.²⁷ mp 300 °C.

9b: mp 221 °C, lit.²⁸ mp 221 °C; ^{13}C NMR ($\text{CDCl}_3/\text{DMSO}-d_6$) δ 165.3, 155.5, 132.8, 129.0 (2), 128.3 (2), 127.8, 127.7, 108.3.

9c: mp 129–131 °C, lit.²⁹ mp 129 °C; IR (KBr) ν 3210, 1751, 1679, 1492, 1475 cm^{-1} ; ^{13}C NMR ($\text{CDCl}_3/\text{DMSO}-d_6$) δ 172.1, 167.7, 152.8, 54.6, 23.6, 14.6.

Formation of Parabanic Acids 12. **11a** or **11b** (500 mg, 2.63 or 4.31 mmol) was treated with 16 mmol of NO_2 as above for 6 h. After workup, the products **12** were obtained quantitatively in spectroscopically (^1H and ^{13}C NMR) pure form.

12a: mp 245 °C, lit.³⁰ mp 247 °C.

12b: mp 214 °C, lit.³¹ mp 214 °C; ^{13}C NMR ($\text{DMSO}-d_6$) δ 158.7, 157.3, 153.6, 130.8, 129.0 (2), 128.6, 126.7 (2).

Formation of 1-Nitrohydantoin (14) and Parabanic Acid 12a. Hydantoin **13** (500 mg, 5.0 mmol) was treated with 490 mg (11 mmol) of NO_2 as above for 12 h. After condensation of excess NO_2 and NO in a cold trap at 77 K (FT-IR detection), 725 mg (100%) **14**, mp 174 °C (lit.³² mp 173–174 °C), was obtained: IR (KBr) ν 1813, 1735, 1566, 1287 cm^{-1} ; ^1H NMR ($\text{DMSO}-d_6$) δ 11.43 (NH), 4.42 (s, CH_2); ^{13}C NMR ($\text{DMSO}-d_6$) δ 166.1, 149.5, 51.9; MS (EI) *m/e* 145 (M^+ , 10), 100 (8), 72 (6), 57 (19), 47 (100). If the same reaction was run at 100 °C for

8 h, 570 mg (100%) of parabanic acid **12a** (and N_2O) was obtained instead of **14**.

Formation of 3-Nitrooxazolidin-2-one (16). Oxazolidin-2-one (**15**) (500 mg, 5.75 mmol) was treated with 6.4 mmol of NO_2 as above for 12 h. After condensation of remaining NO_2 and NO in a cold trap at 77 K, 740 mg of a solid 80/20 mixture of **16** and 3-nitrosooxazolidin-2-one was obtained. Recrystallization from toluene gave 530 mg (70%) of **16**, mp 111 °C (lit.³³ mp 111 °C): IR (KBr) ν 1801, 1746, 1466, 1384, 1352, 1165 cm^{-1} ; ^1H NMR (CDCl_3) δ 4.61 (AA'BB', 2), 3.97 (BB'AA', 2); ^{13}C NMR (D_2O) δ 154.9, 63.1, 40.4. A similar nitrosation with 11 mmol of NO (0.9 bar) for 12 h gave a liquid mixture of 65% 3-nitrosooxazolidin-2-one³⁴ and 35% **15**: ^1H NMR (CDCl_3 , main component) δ 4.54 (AA'BB', 2), 3.73 (BB'AA', 2); ^{13}C NMR (D_2O , main component) δ 155.7, 65.1, 41.1.

Formation of 5-Nitrobarbituric Acids 18. Barbituric acid **17a** (500 mg, 3.91 mmol), 500 mg (3.21 mmol) of **17b**, or 500 mg (2.72 mmol) of **17c** was reacted as above with 490 mg (11 mmol) of NO_2 at an initial pressure of 0.3 bar for 4 h. After condensation of the gases to a cold trap at 77 K, the solid products weighed 694, 687, or 665 mg, and after drying at 80 °C in a vacuum, pure **18a** (676 mg, 100%), **18b** (645 mg, 100%), or **18c** (623 mg, 100%) was obtained. The water content was also determined by TGA (10 K/min) to be 20 (75 °C), 42 (72 °C), or 46 mol % (96 °C), respectively.

18a: mp 183 °C, lit.¹⁷ mp 180–181 °C; IR (KBr) ν 1729, 1651, 1448, 1386, 1297 cm^{-1} ; MS (EI) *m/e* 173 (82, M^+), 135 (11), 134 (25).

18b: mp 148 °C dec, lit.¹⁷ mp 148–149 °C.

18c: mp 116 °C dec, lit.¹⁷ mp 116–117 °C.

Nitration of 4-Hydroxybenzaldehyde (19). 4-Hydroxybenzaldehyde **19** (500 mg, 4.1 mmol) was reacted as above with 490 mg (11 mmol) of NO_2 at an initial pressure of 0.3 bar for 12 h. After evaporation of the gases, the product mixture (685 mg, 100%) contained 82% **20** and 18% **21** according to ^1H -NMR analysis. The mixture was separated by preparative layer chromatography (SiO_2 , EtOAc) to isolate 528 mg (77%) of **20**, mp 143 °C (lit.²⁰ mp 142–143 °C), and 116 mg (17%) of **21**, mp 104 °C: IR (KBr) ν 3420, 2922, 2852, 1736, 1604, 1532, 1464, 1344 cm^{-1} ; ^1H NMR ($\text{CDCl}_3/\text{DMSO}-d_6$) δ 9.89 (s, 1), 8.73 (s, 1), 7.80 (d, 1), 7.07 (d, 1).

Nitration of Vanilline (22). Vanilline (**22**) (500 mg, 3.29 mmol) was treated as **19** above. The reaction mixture (650 mg, 100%) contained 84% **23**, 10% **24**, and 6% **25** according to ^1H -NMR analysis. The mixture was separated by preparative layer chromatography to isolate 526 mg (81%) of **23**, mp 178 °C, lit.³⁵ mp 176 °C; 63 mg (10%) of **24**, mp 137 °C, lit.³⁵ mp 137 °C; and 38 mg (6%) of **25**, mp 210 °C, lit.³⁵ mp 207 °C. The products were also identified by their IR, ^1H -NMR, and MS data.

Formation of 9-Methyl-10-nitroanthracene (27). 9-Methylanthracene (**26**) (200 mg, 1.04 mmol) was reacted with 296 mg (6.4 mmol) of NO_2 as above for 12 h. After removal of the gases, 245 mg (100%) of **27**, mp 201 °C, lit.²¹ mp 203–205 °C, was obtained and characterized by its IR, ^1H -NMR, and MS data.

Reaction of Solid Anthracene (28) with Gaseous NO_2 . Anthracene (**28**) (scales) (250 mg, 1.40 mmol) was reacted with 296 mg (6.4 mmol) of NO_2 at an initial pressure of 0.3 bar at room temperature or at 0.03 bar initial pressure at -10 °C. Product analysis was done by ^1H NMR in CDCl_3 using known spectra of **29** (*cis* and *trans*),²² **31**, and **32**. **30** (stereochemistry unknown) exhibited characteristic singlets at δ 6.67 and 5.64.³⁶ Upon chromatography only **30** and **32** survived and could be isolated. After standing of CDCl_3 solutions containing **29** for several days, 9-nitroanthracene was detected by ^1H NMR. At 28% conversion of **28** at room temperature, the composition of the products was 14% *trans*-**29c**, 17% *cis*-**29**, 21% **30**, 45%

(33) Franchimont, A. P. N.; Lublin, A. *Recl. Trav. Chim. Pays-Bas* **1902**, 21, 49.

(34) Gabriel, S. *Chem. Ber.* **1905**, 38, 2404.

(35) Hynning, P.-A.; Remberger, M.; Neilson, A. H. *J. Chromatogr.* **1989**, 467, 99.

(36) An *aci*-dinitro derivative similar to **30** has been described in a reduction of 9-nitroanthracene: Takikawa, Y.; Abe, T.; Sato, R.; Takizawa, S. *Chem. Lett.* **1980**, 25.

(27) Carrington, H. C.; Waring, W. S. *J. Chem. Soc. C* **1950**, 354.

(28) Stuckey, R. E. *J. Chem. Soc.* **1949**, 207.

(29) Harries, C.; Weiss, M. *Liebigs Ann. Chem.* **1903**, 327, 355.

(30) Laursen, P. H. *J. Org. Chem.* **1957**, 22, 274.

(31) Bergmann, M.; Delis, D. *Liebigs Ann. Chem.* **1927**, 458, 86.

(32) Stuckey, R. E. *J. Chem. Soc.* **1947**, 331.

31, and 3% **32**. After 3 h at 25 °C and complete conversion of **28**, the reaction mixture contained 75% **31**, 20% **32**, 4% *cis*-**29**, and less than 1% **30**. At -10 °C the transformation of **28** was 35% after 12 h. The composition of the products was 18% *trans*-**29**, 19.5% *cis*-**29**, 29% **30**, 17% **31**, and 16.5% **32**.

Nitration of Tetraphenylethylene (33). (a) **Without Drying Agent.** Tetraphenylethylene (**33**) (300 mg, 0.90 mmol) was reacted with 16 mmol of NO₂ at an initial pressure of 0.3 bar for 12 h. The solid product was wet. After evaporation of the gases, the dry reaction mixture (420 mg) was separated by preparative layer chromatography on 200 g of SiO₂ with CH₂Cl₂. Then 27 mg (7%) of **33** and 43 mg (15%) of *p*-mononitro-, 110 mg (34%) of *p*-trinitro-, and 170 mg (44%) of *p*-tetranitro compound **34** were eluted and characterized by their proper molecular ions in the mass spectra.

(b) **With Drying Agent.** **33** (800 mg, 2.41 mmol) was mixed with 800 mg of MgSO₄·2H₂O. After 12 h of reaction with 710 mg (15.4 mmol) of NO₂ at an initial pressure of 0.3 bar and rt, the excess gas and NO were condensed in a cold trap at 77 K and analyzed by gas phase FT-IR (NO/NO₂ ratio was 10/2). The product was extracted from the drying agent

with CH₂Cl₂, yielding 1.17 g (95%) of pure **34**, mp 300–302 °C, lit.²⁵ mp 298–299 °C: IR (KBr) ν 1598, 1518, 1342 cm⁻¹; ¹H NMR (CDCl₃) δ 8.05 (d), 7.18 (d); MS (EI) *m/e* 512 (100, M⁺), 496 (2), 482 (4), 408 (4), 373 (4), 327 (6), 326 (8), 315 (6), 287 (4), 162 (6).

For larger runs the use of a flow apparatus is advisable, which allows for circulating of the gas and admixing of the calculated amount of oxygen to oxidize the NO formed for use in the running reaction.

Acknowledgment. We thank Mrs. M. Juniel and Mrs. E. Jaskulska for technical assistance. Dr. M. Moebus, Universitaet Stuttgart, Dr. J. Schreuer, Universitaet zu Koeln, and W. Saak are thanked for the determination of the Miller indices of **11a**, **28**, **1a**, and **33**. M. Haak, U. Pogodda, and T. Marquardt are thanked for the maintenance of our various computer facilities.

JO950025U